

Software for multi-average processing in neonatal cardiac imaging

Andreia S. Gaspar^{1,2}, David J. Cox¹, Alan M. Groves^{1,3}, and Anthony N. Price¹

¹Centre for the Developing Brain, King's College London, London, United Kingdom, ²Instituto de Biofísica e Engenharia Biomédica, Faculdade de Ciências, Universidade de Lisboa, Lisboa, Portugal, ³Department of Pediatrics, Weill Cornell Medical College, New York, United States

Purpose: Cardiac MRI using steady state free precession (SSFP) provides excellent imaging efficiency and contrast. The technique has recently been applied to preterm infants providing more robust assessment of cardiac function¹. In these small subjects multiple signal averages are required to maximize signal to noise ratio (SNR)². Acquisition is performed free-breathing and unsedated, often leading to individual averages displaying respiratory and bulk motion artefacts, as well as differences in contrast and spatial location. If all image averages are incorporated equally into the final dataset without further processing – as occurs in standard scanner reconstruction - the resulting image is often sub-optimal. Guided processing of the separate image averages could improve the final composite image, facilitating easier and more accurate analysis of cardiac structure and function.

Methods: Software was developed to analyse and process individually reconstructed image averages from a cine stack acquisition, optimized for neonatal scanning. The software incorporated: image registration, intensity analysis and image average rejection processes (Figure 1). Initial rigid-body image registration by cross-correlation³ aligned slice averages at end-diastole to allow comparison of intensity histograms. Intensity analysis calculated a quality index, constituting measures of entropy, cross-correlation, and histogram parameters of whole-heart, blood pool and myocardial regions. Parameters indicating intensity differences between blood pool and myocardium were assigned greater weight in the final index, e.g. histogram intersection area between regions. Image averages with a high index score (>10) were excluded for each slice; a second iterative rigid-body registration step followed. The spatial transformations and averages to be excluded were extrapolated to all 20 temporal frames. The final images were exported for segmentation and analyses of cardiac function.

The software was applied to 8 neonatal cardiac studies deemed to be of poor quality due to motion artefact. Median corrected gestational age was 34 weeks (31-35 weeks), median weight at scan 1650 g (920-2080 g). Data was acquired on a 3T Philips Achieva scanner using an 8-channel paediatric receive coil. Infants were scanned unsedated with routine clinical monitoring; a 10 slice short axis stack of 4 or 8 signal averages was acquired using retrospectively-gated SSFP. Cardiac cine data was reconstructed offline in Matlab R2012a to provide images for each signal average. Left ventricle (LV) segmentation was performed in Segment version 1.9 R3845 (<http://segment.heidelberg.se>), before and after the software application. LV mass (LVM), end-diastolic volume (EDV), end-systolic volume (ESV), stroke volume (SV) and ejection fraction (EF) were determined and normalised to the body mass. A subjective evaluation of data quality improvement was performed using a 2-person blinded analysis; the 9 apical slices of each pre- and post-processed dataset were assigned a quality score of 1-5 based on the evaluator's perceived ease of segmentation.

Results: An improvement in image quality was observed after processing the data with the developed software. The first rigid-body registration process increased the sharpness of the endocardial border in cases of marked movement between individual average images. The quality indices calculated were consistent with the observed image quality characteristics for the chosen threshold. Intensity parameters from the entire heart region of interest (ROI) rapidly determined signal averages of very poor image quality, which should be excluded from the final multi-averaged image. The evaluation of the blood pool and myocardium ROI histograms identified the contrast characteristics of the endocardial border. The presentation of all processing parameters in a single graphical interface allowed the user to evaluate the results of each stage in real time, promoting an informed decision of which images should be included to improve contrast. Although the exclusion of averages from the image combination offsets the SNR gains of signal averaging, the improvement in contrast facilitates more accurate segmentation and therefore more robust quantification. The nature of retrospectively-gated sequence allowed the analyses of the end-diastolic phases to be extrapolated to all other cardiac phases; extrapolation without further user interaction or processing gave a similar improvement in image quality at end-systole. Mean \pm standard deviation of subjective evaluation scores, for pre and post-processed datasets, were 3.3 ± 1.0 and 3.7 ± 0.9 ($p < 0.05$), indicating improved image quality after post-processing. LV segmentation performed on the post-processed stacks showed a statistically-significant decrease in the measured LVM 2.53 ± 0.44 g/kg vs 2.88 ± 0.67 g/kg ($p < 0.05$). The decrease in measured LVM is likely to result from clearer definition of epicardial border primarily. Comparison of EDV and ESV, and cardiac functional parameters (SV and EF) did not reveal any significant differences for this cohort.

Conclusion: Cardiac MRI of newborn infants could prove to be an important tool in assessing cardiac function¹, but standard acquisition techniques used in adult CMR are prone to infant motion. Automatic image registration of signal averages appears advantageous, whilst the use of the described index assists the user in the decision to exclude individual averages. This software enables easy recovery of data that would not otherwise be thought fit for evaluation. This could prove important in future research studies or clinical trials that investigate cardiac anatomy and function in this unique and valuable cohort.

References: 1. Groves AM, et al. Arch Dis Child Fetal Neonatal Ed. 2011; 96(2):F86-91.; 2. Price AN, et al. Magn Reson Med. 2013; 70:776-784.; 3. Guizar-Sicairos M, Thurman ST. Opt Lett. 2008; 33(2):156-8; **Acknowledgement:** MRC strategic funds and GSTT BRC.

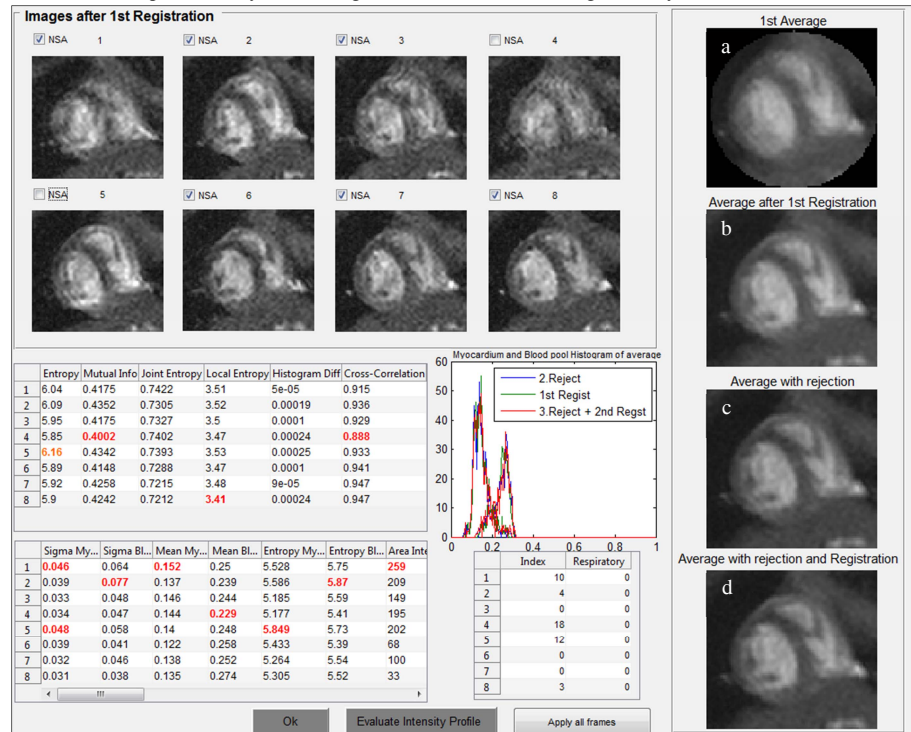


Figure 1 – Software interface for multi-average image processing. Mid short-axis images at end-diastole: a) initial image; b) after first registration; c) after alignment and individual sample rejection; d) final averaged image. Individual averages with respective intensity indexes are presented. Histograms of blood pool and myocardial regions of the images b (blue), c (green) and d (red) are presented.